

**Electronic Supplementary Information for:**

**Pumping Fluids in Microfluidic Systems Using the Elastic Deformation  
of Poly(dimethylsiloxane)**

Douglas B. Weibel,<sup>\*a,b</sup> Adam C. Siegel,<sup>b</sup> Andrew Lee,<sup>b</sup> Alexander H. George,<sup>b</sup> and  
George M. Whitesides<sup>\*b</sup>

<sup>a</sup> *Department of Biochemistry, University of Wisconsin-Madison*

*433 Babcock Drive, Madison, WI, 53706, U.S.A.*

<sup>b</sup> *Department of Chemistry and Chemical Biology, Harvard University*

*12 Oxford St., Cambridge, MA, 02138, U.S.A.*

\* Electronic addresses: [weibel@biochem.wisc.edu](mailto:weibel@biochem.wisc.edu); [gwhitesides@gmwgroup.harvard.edu](mailto:gwhitesides@gmwgroup.harvard.edu)

**Materials.** We used a ratio of 10:1 of the base/curing agent for PDMS; the Young's modulus of this material after curing is 2.4 mPa (value reported by Dow Corning). In addition to the compartments fabricated and studied in this paper, we also explored two approaches to increase the rate of flow of fluids out of PDMS compartments: i) we modified the elastic modulus of the PDMS by increasing the concentration of crosslinker to 20-40%; and ii) we cured and bonded a layer of polyurethane (NOA 81) to the top surface of the PDMS and made the roof of the compartments more rigid. Both of these modifications increased the rate of flow out of compartments (data not shown).

**Volume/pressure relationship in pressurized compartments.** To determine the relationship between the volume and pressure of fluid introduced into a compartment, we prototyped three microfluidic systems that share a similar design but have different critical dimensions. Each system contained a central, cylindrical compartment connected to an inlet channel and an outlet channel attached to a series of adjacent circular reservoirs. This specific design was chosen because it made it possible for us to measure the volume of fluid released from a compartment over time quickly by counting the number of reservoirs filled with liquid; this characteristic was particularly useful in experiments where we measured flow rates of fluid.

A valve was incorporated into each inlet and outlet channel; the channels were connected to a compartment. All three compartments we tested had different critical dimensions (diameter, height) and a total volume of 0.5  $\mu\text{L}$ . Design A consisted of an

inlet channel (24- $\mu$ m wide, 24- $\mu$ m tall, 7-mm long) connected to a circular compartment (5.2-mm diameter, 24- $\mu$ m tall, 0.5- $\mu$ L volume) with a short outlet channel (24- $\mu$ m wide, 24- $\mu$ m tall, 7-mm long) connected to a series of 24 interconnected circular reservoirs (2.4-mm wide, 24- $\mu$ m tall, 0.1- $\mu$ L volume). Design B consisted of an inlet channel (18- $\mu$ m wide, 18- $\mu$ m tall, 7-mm long) connected to a circular compartment (6-mm diameter, 18- $\mu$ m tall, 0.5- $\mu$ L volume) with a short outlet channel (18- $\mu$ m wide, 18- $\mu$ m tall, 7-mm long) connected to a series of 24 interconnected circular reservoirs (2.8-mm wide, 18- $\mu$ m tall, 0.1- $\mu$ L volume). Design C consisted of an inlet channel (12- $\mu$ m wide, 12- $\mu$ m tall, 7-mm long) connected to a circular compartment (7.3-mm diameter, 12- $\mu$ m tall, 0.5- $\mu$ L volume) with a short outlet channel (12- $\mu$ m wide, 12- $\mu$ m tall, 7-mm long) connected to a series of 24 interconnected circular reservoirs (3.2-mm wide, 12- $\mu$ m tall, 0.1- $\mu$ L volume).

When compartments A-C were filled with liquid (4  $\mu$ L) under pressure, the largest deformation (deflection) of PDMS occurred at the ceiling rather than at the walls; the thickness of the PDMS in the ceiling and walls was 4 mm and 15 mm, respectively. We used the same thickness of the layer of PDMS above the compartments (4 mm) in all of the microfluidic systems we studied in this paper; compartments with a layer of PDMS <4 mm also worked (data not shown).

We filled compartments A-C (volume, 0.5  $\mu$ L) with 0-30  $\mu$ L of an aqueous solution of dye (to make it easy to visualize the liquid), closed the valves on the inlet and outlet microfluidic channels to isolate the fluid, and measured the pressure in the compartments. To measure the pressure, we drilled a small hole in the inlet channel

between the valve and the compartment during the fabrication of the microfluidic system, and inserted a piece of polyethylene tubing (PE-60). The tubing was connected to an electronic pressure sensor (Honeywell, model ASDX100G24R) that was powered by a 5 V supply (BK Precision), and the voltage from the sensor was measured using a digital multimeter (Fluke 87III). To determine the pressure-to-voltage conversion for the pressure sensor, we measured the voltage at a series of known pressures, plotted the voltage/pressure data, and fit the data using a linear function (Figure S1). We filled compartments with different volumes of aqueous solutions of dye using a syringe pump, measured the voltage, and converted the data to pressure using the voltage/pressure plot.

The maximum pressure that these compartments could withstand before the layer of PDMS separated from the glass slide was 400-500 kPa (60-70 psi). Figure S2 shows the relationship between the pressure/volume of liquid in cylindrical compartments that have different critical dimensions and the same volume. As the surface area of the ceiling of the compartment decreased, the pressure per unit volume of fluid increased. Using the volume of fluid infused into the compartments, and estimating the resistance of the outlet channel using laminar pressure drop equations,<sup>S1,S2</sup> users can predict the initial rate of flow of fluid from compartments (see text below).

In experiments in which we studied the volume/pressure relationship of fluids in compartments, we estimated the resistance of the outlet channels by making the hydraulic analogy: that is, Poiseuille's law corresponds to Ohm's law for electrical circuits ( $V=IR$ ). In this analogy, the pressure drop  $\Delta P$  is analogous to the voltage,  $V$ , the rate of fluid flow  $\phi$  is analogous to the current,  $I$ , and the resistance,  $R$ .

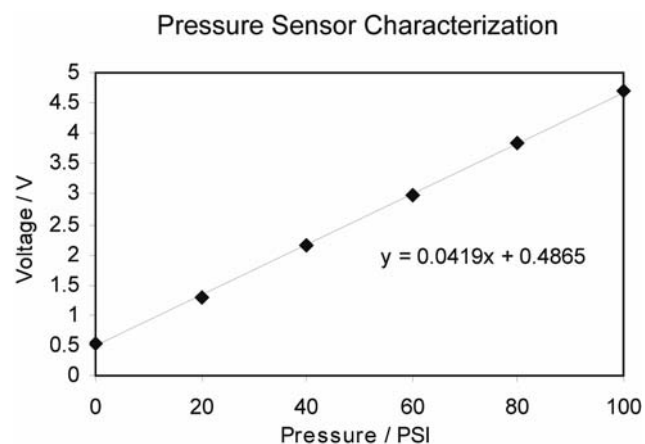


**Figure S1.** Pressure-to-voltage conversion for the pressure sensor. To determine the pressure in compartments, we measured the voltage at a series of known pressures, plotted the voltage/pressure data, and fit the data using a linear function.

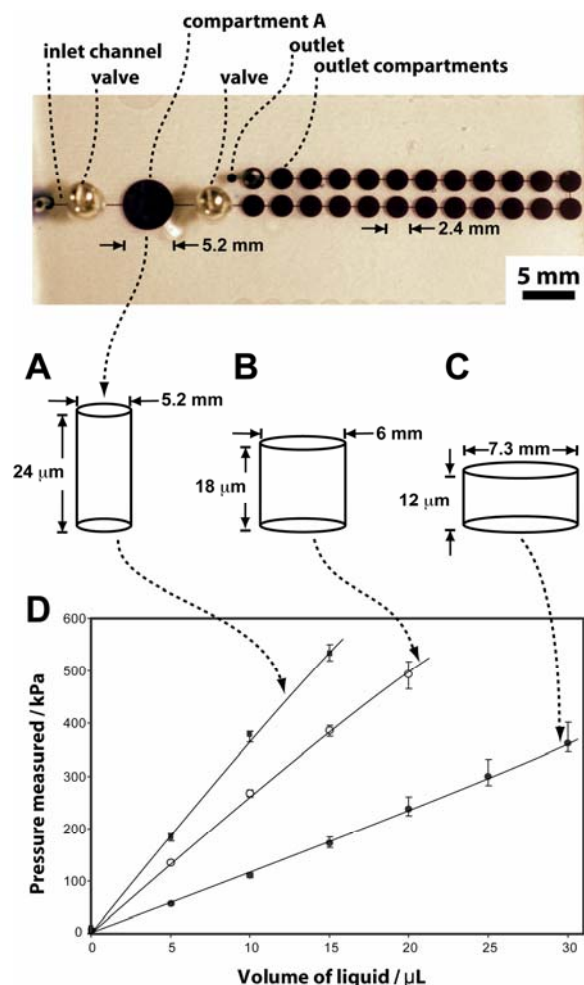


**Figure S2.** The relationship between the pressure and volume of fluids in cylindrical compartments. All three compartments we tested (A-C) had a volume of 0.5  $\mu\text{L}$ . The top image shows a microfluidic system containing design A that was filled with ink to make the channels easy to visualize. A-C) Schematic diagrams and critical dimensions of compartments A-C; these compartments are not drawn to scale. D) A plot showing the relationship between the pressure and volume in the compartments. We filled compartments A-C with 0-30  $\mu\text{L}$  of an aqueous solution of dye, isolated the fluid, and measured the pressure in the compartments. We averaged the pressure measured at

each volume of fluid over five duplicate experiments for each compartment: A (■), B (○), and C (●). The error bars represent minimum/maximum values of the pressure. Equation S1 defines the resistance in a channel with a rectangular cross section, where  $w$  is the width of a channel (mm),  $h$  is the height of a channel (mm),  $L$  is the length of a channel (mm),  $\mu$  is the viscosity of the fluid (in these experiments, water, which has a viscosity of  $8.9 \times 10^{-4}$  Pa·s at 25 °C).

$$R = \frac{12\mu L}{wh^3} \left[ 1 - \frac{h}{w} \left( \frac{192}{\pi^5} \sum_{n=1,3,5}^{\infty} \frac{1}{n^5} \tanh\left(\frac{n\pi w}{2h}\right) \right) \right]$$

#### Equation S1

In the channels described in this paper,  $w=h$ , and Equation S1 can be approximated by  $R=6.84\mu L/h^4$ . Estimating the hydraulic resistance by using only the first three terms of the sum, we calculate a resistance of 120, 379, and 1920 kPa·s/mm<sup>3</sup> for compartments A-C.

To estimate the initial velocity of fluid flowing out of compartments A-C, we used the fluidic analogy to Ohm's law, where  $V=IR$ . Values for the hydraulic resistance,  $R$ , were calculated above, and the pressure of the compartments,  $V$ , was determined as described below; we used values of  $V$  of 150, 110, and 47 kPa for compartments A-C, respectively. The initial velocity of fluid pushed out of compartments A-C was 1.25, 0.3, and 0.02  $\mu\text{L/s}$ , respectively.

Since the rate of flow and volume of fluid released from a compartment is ultimately controlled by the valves, we treat the compartments in this paper as

reservoirs for the storage and delivery of volumes of fluids that are chosen by the user; we do not characterize them as components for dispensing precise volumes of fluids per se. We envision the deployment of these components in portable devices in which an *excess* of fluid is stored in compartments. Compartments will ideally be chosen to have the largest aspect ratio possible so that the flow rate of fluid out of the compartments is high and can be decreased, if necessary, by controlling the valves. An analysis of how the rate of flow of fluids from compartments changes over time as a function of the parameters for each experiment (e.g. the volume of fluid, the critical dimensions of the compartment, or the resistance of the outlet channel) is beyond the scope of this paper. The equations that describe the deformation of solids can be found elsewhere.<sup>S3,S4</sup>

To demonstrate the rate of flow of fluid out of compartments, we filled A-C with 4  $\mu\text{L}$  of fluid using a syringe pump. After closing the valves on the inlet and outlet channels for 1 min to check for leaks, we opened the valve on the outlet channel and measured the volume of fluid released from the compartments into the outlet channels over time. We repeated the experiment with all three microfluidic geometries and averaged the rate of flow of fluid over five duplicate experiments. The data are presented in Figure S3. Design A had a ceiling with the smallest surface area ( $21 \mu\text{m}^2$ ) of the three designs and released liquid more rapidly than the others: ~65% of the volume of liquid was released after 20 sec. In contrast, design C had a ceiling with the largest surface area ( $42 \mu\text{m}^2$ ) of the three designs and released liquid most slowly: ~65% of the volume of liquid was released after 160 sec.

To demonstrate that the relationship between the flow rate and the surface area of the ceiling is independent of the shape of the compartment, we repeated the



experiments with three rectangular-shaped compartments that had the same volume and different vertical and horizontal dimensions (Figure S4).

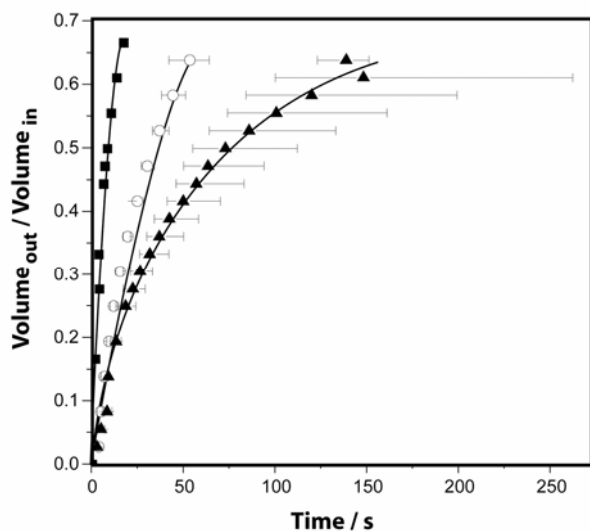


**Figure S3.** The relationship between the critical dimensions of compartments and the volume of fluid released over time. We filled compartments A-C (Figure 4) with 4  $\mu\text{L}$  of black ink, stored the fluid in the compartments for 5 min, released the liquid by opening the valve on the outlet channel, and measured the volume of fluid released over time. The plot shows the volume of fluid released over time for compartment A (■), B (○), and C (△); the data points represent the average of five measurements, and the error bars show minimum/maximum values of the rate of flow.

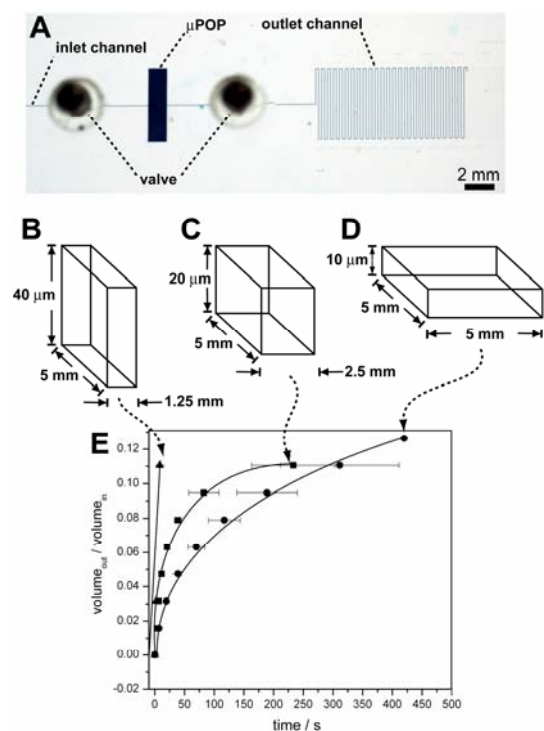


**Figure S4.** Measuring the relationship between the geometry of compartments and the volume of fluid released over time. The three microfluidic systems consisted of an inlet channel (125  $\mu\text{m}$  wide, 11 mm long) connected to a rectangular compartment (0.25  $\mu\text{L}$  volume, labeled ‘ $\mu\text{POP}$ ’) with a serpentine outlet channel (125  $\mu\text{m}$  wide, 20 cm long); both channels had a TWIST valve. A) An image of compartment B filled with black ink; the outlet channel was partially filled with ink. Each compartment was rectangular with the following dimensions: B (1.25 mm wide, 5 mm long, 40  $\mu\text{m}$  tall), C (2.5 mm wide, 5 mm long, 20  $\mu\text{m}$  tall), and D (5 mm wide, 5 mm long, 10  $\mu\text{m}$  tall). We filled the compartments with ink (5  $\mu\text{L}$ ), stored the ink under pressure for 5 min, opened the valve

on the outlet channel, and measured the volume released over time. E) A plot of the volume of fluid versus time; error bars show the standard deviation in the mean volume measured over four duplicate experiments with the same device.

The compartments were connected to long, serpentine outlet channels; with these devices, we observed a similar trend to experiments with cylindrical compartments.

**Adsorption of reagents on PDMS.** A possible complication of using PDMS for this application is that small molecules and proteins can adsorb on the surface of PDMS from solution; this adsorption has the potential to reduce the concentration of reagents in solution,<sup>S5</sup> and may pose a problem when an assay requires specific concentrations of reagents. We anticipated that freezing devices in which pressurized compartments are filled with aqueous solutions of reagents would minimize the adsorption of reagents on PDMS because of the barrier to the diffusion of reagents in a solid (ice). To confirm that freezing prevents the adsorption of reagents on surfaces during storage, we measured the change in the concentration of solutions of IgG and avidin stored in PDMS compartments at -20 °C over time.

Figure S5 shows how the concentration of IgG labeled with fluorescein isothiocyanate (IgG-FITC) and avidin labeled with tetramethylrhodamine isothiocyanate (avidin-TRITC) change over time during storage in PDMS at -20 °C. We filled several dozen microfluidic devices containing compartments (volume, 0.8  $\mu$ L) with 4  $\mu$ L of a solution of protein (either 1 mg/mL avidin-TRITC and 2 mg/mL IgG-FITC in 50 mM phosphate-buffered saline, pH 7.0), isolated the fluid under pressure using valves on the

inlet and outlet channels, and immediately stored the devices in a Ziplock bag at  $-20\text{ }^{\circ}\text{C}$ . We thawed out devices over time, released the fluid into an outlet channel, collected  $2\text{ }\mu\text{L}$ , and measured the concentration of protein using a spectrophotometer. We observed that over 16 days the concentration of protein remained approximately constant.

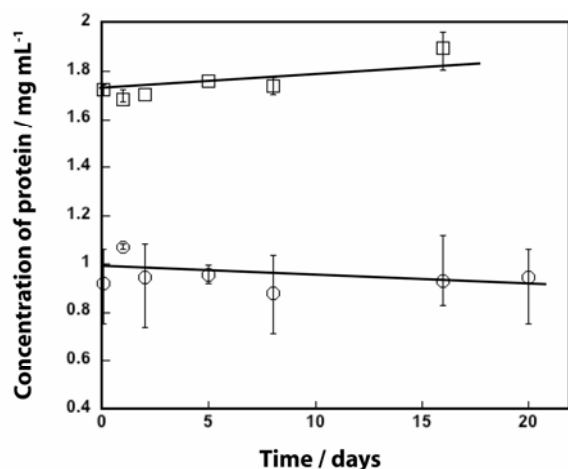


**Figure S5.** Adsorption of proteins on PDMS during storage at  $-20\text{ }^{\circ}\text{C}$  in compartments.

We used two different proteins for this experiment: avidin-TRITC ( $\circ$ ,  $1\text{ mg/mL}$ ) and IgG-FITC ( $\square$ ,  $2\text{ mg/mL}$ ). To measure the concentration of protein in solution we warmed devices to  $25\text{ }^{\circ}\text{C}$ , released the fluid from the compartment into an outlet, and measured the absorbance of  $2\text{ }\mu\text{L}$  of liquid at a wavelength of either  $488\text{ nm}$  (IgG-FITC) or  $550\text{ nm}$  (avidin-TRITC). The concentration of protein was determined from a standard curve of concentration versus absorbance. Each data point represents the mean concentration from three replicate experiments with different compartments; error bars represent minimum/maximum values of concentration.

To correlate absorbance measurements with concentration of protein we created standard curves for both IgG-FITC and avidin-TRITC (Figure S6, S7); both proteins were purchased from Sigma Aldrich. The concentration of protein solutions stored at - 20 °C in PDMS compartments were measured as described in the text using 2  $\mu$ L of liquid and a NanoDrop ND-1000 spectrophotometer (Table S1).

Time (hr)	Mean absorbance ( $\lambda$ , 550 nm) of avidin-TRITC	Mean absorbance ( $\lambda$ , 488 nm) of IgG-FITC
1	0.074	0.244
24	0.086	0.238
48	0.076	0.241
120	0.077	0.250
192	0.071	0.246
384	0.075	0.269
480	0.076	

**Table S1.** Mean values of the concentration of protein in solution during storage for different periods of time. Each point represents the mean concentration of protein averaged over at least three different devices.

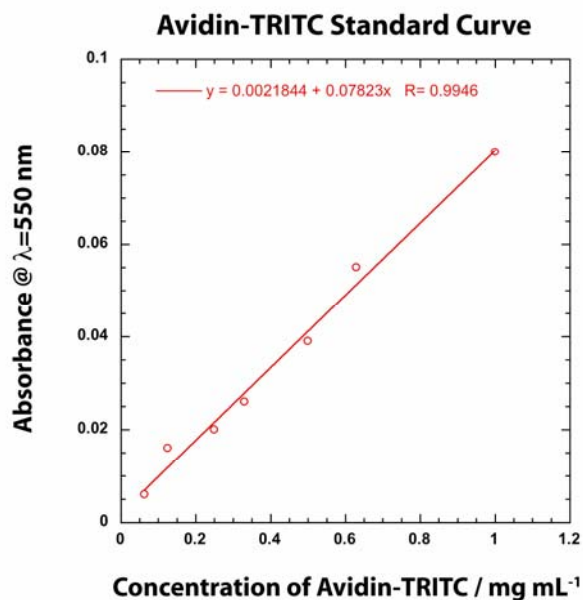


**Figure S6.** Plot of absorbance versus concentration for avidin-TRITC (standard curve).

Each data point represents the mean value of measurements made in triplicate. The points were fit to a linear equation (red) to calculate the slope and R-value.

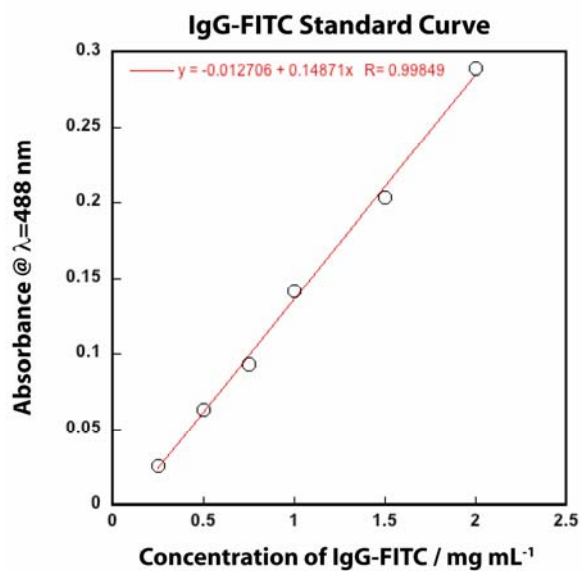


**Figure S7.** Plot of absorbance versus concentration for IgG-FITC (standard curve). Each data point represents the mean value of measurements made in triplicate. The points were fit to a linear equation (red) to calculate the slope and R-value.

**Liquid Pumps for Moving Fluids.** We found that we were able to produce small PDMS microfluidic devices (surface area,  $\sim 1\text{-}2\text{ cm}^2$ ) with valves that could be used to store and pump different reagents under pressure in individual compartments. Pressurizing multiple compartments with different reagents was time-consuming and proved to be technically challenging. We therefore explored an alternative approach to manipulating multiple reagents in portable microfluidic devices.

As a pilot study, we fabricated a microfluidic system in PDMS with a central compartment (15-mm diameter, 25- $\mu\text{m}$  tall, 4.5- $\mu\text{L}$  volume) supported by 32 PDMS posts (200- $\mu\text{m}$  wide, 25- $\mu\text{m}$  tall), with four outlet channels (200- $\mu\text{m}$  wide, 25- $\mu\text{m}$  tall, 7.7-mm long) positioned symmetrically around the circular compartment (Figure S8); the slab of PDMS was bonded to a glass slide. The posts were included to prevent the ceiling of the chambers from collapsing when the slab of PDMS was bonded to a glass slide. The outlet channels were each connected to circular reservoirs (6-mm diameter, 25- $\mu\text{m}$  tall, 0.75- $\mu\text{L}$  volume) reinforced with 32 PDMS posts (200- $\mu\text{m}$  wide, 25- $\mu\text{m}$  tall), that in turn, had an inlet channel (200- $\mu\text{m}$  diameter, 25- $\mu\text{m}$  tall, 7-mm long) and a serpentine outlet channel (200- $\mu\text{m}$  diameter, 25- $\mu\text{m}$  tall, 60-mm long); all of the channels in the device had integrated TWIST valves. We filled the central compartment with an organic fluid—perfluoromethyldecalin (PFMD) or silicone oil (DC 200)—that was immiscible with water and swelled PDMS minimally.<sup>S6</sup>

Figure S8 shows a device that demonstrates this concept; we refer to this as a ‘pump’ because it uses an immiscible liquid under pressure to push a secondary liquid from the reservoir in which it is stored.



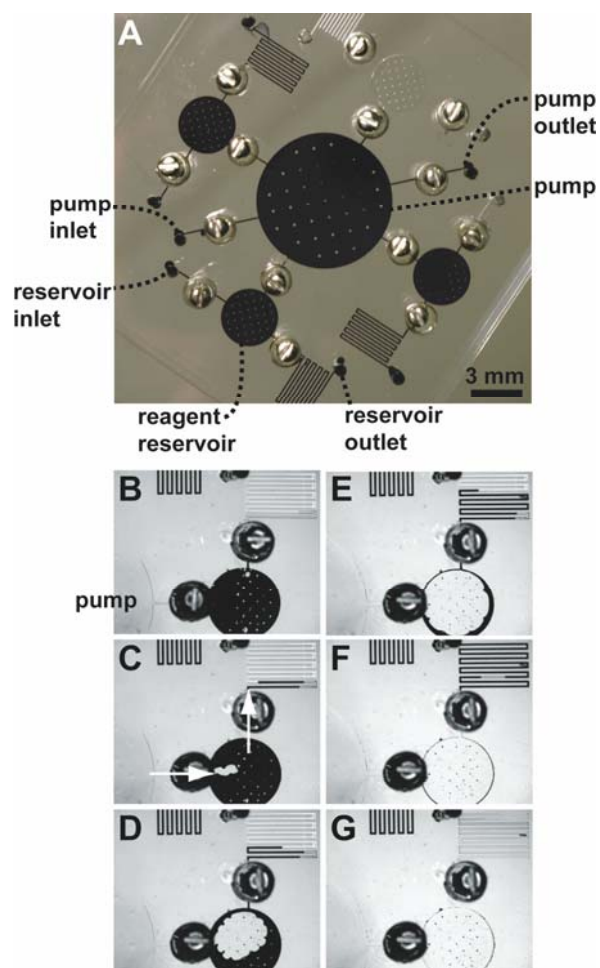


**Figure S8.** Liquid pumps for manipulating fluids in microfluidic channels. A) An image of a device with critical dimensions described in the text above. The compartment and three of the reservoirs were filled with ink to make them easy to visualize; the reservoir at the top of the image was empty. B) The ink in the compartment was removed and the compartment was filled with PFMD (20  $\mu$ L) and stored under pressure by closing the TWIST valves on the outlet channels. The top reservoir was filled with black ink (1  $\mu$ L), and the valve on the inlet channel was closed; the valve on the outlet serpentine channel remained open. C) The valve in between the compartment and the reservoir was opened; the image was taken 2 sec after opening the valve. The white arrows show the

direction of the flow of the fluids: PFMD flowed into the reservoir and pushed ink into the serpentine channel. Images D-G were acquired in 2 sec intervals. After 10 sec the PFMD pushed all of the ink out of the reservoir and to the outlet hole; the serpentine channel had filled with PFMD.

The compartment and three of the reservoirs and their inlet and outlet channels were filled with black ink to make them easy to visualize. A fourth reservoir—located at the top of the image—was empty; this reservoir was used in the experiment shown in frames B-G. We removed the ink in the compartment before starting the experiment, by applying a vacuum at the outlet. The compartment was subsequently filled with 20  $\mu\text{L}$  of PFMD using a syringe pump and the fluid was stored by closing the valves on the inlet/outlet channels. The reservoir at the top of Figure S8A was filled with one volume of black ink (1  $\mu\text{L}$ ) using a syringe pump connected to the inlet channel, and the valve on the inlet channel was closed; the valve on the outlet channel remained open and the channel was empty. When the valve between the compartment and the reservoir was opened, PFMD flowed into the reservoir pushing ink through the serpentine outlet channel.

This example demonstrates the use of a single, central compartment filled with an organic solvent to pump fluids in channels or reservoirs connected to the compartment. Silicone oil and PFMD are optimal solvents for filling compartments that serve as central pumps because they: i) are immiscible with water; ii) swell PDMS minimally; iii) are relatively inexpensive; and iv) have a higher boiling point and evaporate more slowly than water.

**Liquid-air-liquid systems for pumping fluids.** A related approach for manipulating fluids in channels uses a central compartment filled with water to push a plug of air into

a reservoir filled with liquid; the plug of air displaces the liquid in the reservoir through an outlet channel. To test this idea, we fabricated the device shown in Figure S9.

The device contained an inlet channel (200- $\mu\text{m}$  wide, 25- $\mu\text{m}$  tall, 21-mm long) connected to a compartment (4 mm-wide, 25- $\mu\text{m}$  tall, 0.3- $\mu\text{L}$  volume); the compartment was attached to a serpentine central channel (200- $\mu\text{m}$  wide, 82-mm long, 25- $\mu\text{m}$  tall, 0.4- $\mu\text{L}$  volume) connected to a fluidic reservoir (4 mm-wide, 25- $\mu\text{m}$  tall, 0.3- $\mu\text{L}$  volume). The reservoir had an inlet channel (200- $\mu\text{m}$  wide, 25- $\mu\text{m}$  tall, 4.8-mm long) and a serpentine outlet channel (200- $\mu\text{m}$  wide, 82-mm long, 25- $\mu\text{m}$  tall, 0.4- $\mu\text{L}$  volume); each channel had an integrated TWIST valve. We filled the compartment with 3  $\mu\text{L}$  of black ink and stored the liquid under pressure by closing the TWIST valves on the inlet and outlet channels. We filled the reservoir with 0.3  $\mu\text{L}$  (one volume) of ink and closed the valves on the connecting channels. The central serpentine channel contained air.

When the valves connecting the compartment to the reservoir, and the valve on the outlet channel of the reservoir were opened, ink flowed out of the compartment and displaced the air plug in the central serpentine channel. The plug of air was pushed into the reservoir and displaced ink into the serpentine outlet channel. The images in Figure S9 demonstrate the principle of using a compartment pressurized with fluid push plugs of air that displace fluid in reservoirs connected to the compartment. It should be possible to connect multiple reservoirs to a single ‘pump’ via channels air-filled microfluidic channels.

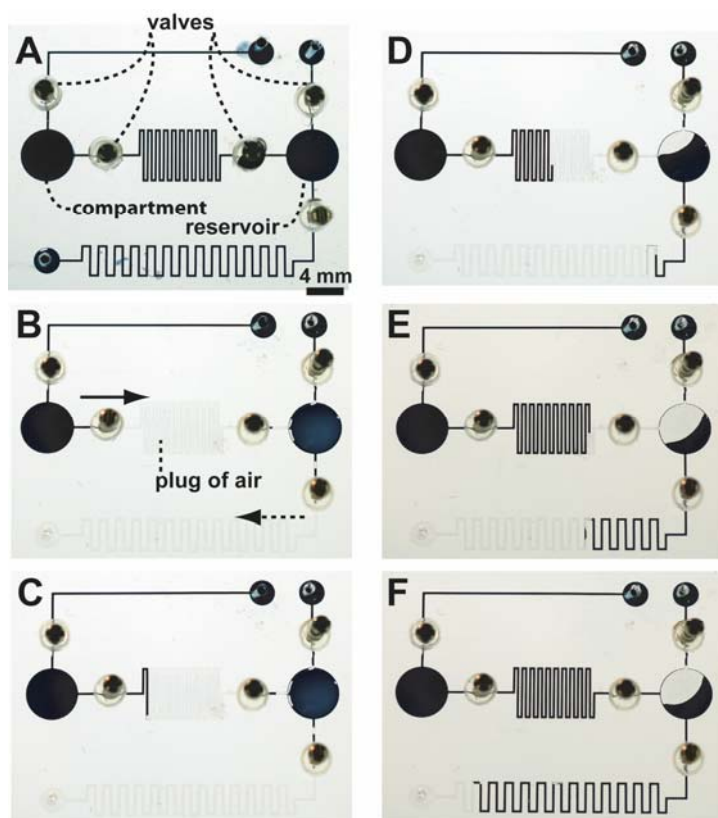


**Figure S9.** Liquid/air/liquid systems for manipulating fluids. A) An image of the device filled with black ink to make the channels, compartment, and reservoir visible. B) The compartment was filled with ink (3  $\mu\text{L}$ ) and the liquid was stored under pressure by closing the TWIST valves on the inlet and outlet channels. The reservoir was filled with ink (0.3  $\mu\text{L}$ ) and the valves on the connecting channels were closed. The central serpentine channel was empty. B) The valves connecting the compartment to the central serpentine channel, the central serpentine channel to the reservoir, and the reservoir to the outlet serpentine channel were opened. The bold arrow depicts the direction of the flow of ink out of the compartment and the dashed arrow shows the flow of ink out of the reservoir. C) An image acquired 3 sec after opening the valves. Ink flowed out of the compartment, pushed the plug of air from the central serpentine channel into the

reservoir. D) After 6 sec. The plug of air pushes ink out of the reservoir into the outlet serpentine channel. E) After 9 sec. F) After 12 sec.

## References

- S1. D. J. Beebe, G. A. Mensing and G. M. Walker, *Annu. Rev. Biomed. Eng.*, 2002, **4**, 261-286.
- S2. N. A. Mortensen and H. Bruus, *Phys. Rev. E*, 2006, **74**, 017301-1–017301-4.
- S3. See, for example: R. P. Feynman, R. B. Leighton and M. Sands, in *The Feynman Lectures on Physics*, Addison-Wesley: Reading, MA, 1989, Chapter 38.
- S4. E. P. Kartalov, A. Scherer, S. R. Quake, C. R. Taylor and W. F. Anderson, *J. Appl. Phys.* 2007, **101**, 06405/1-064505/4.
- S5. M. W. Toepke and D. J. Beebe, *Lab Chip* 2006, **6**, 1484-146.
- S6. J. N. Lee, C. Park and G. M. Whitesides, *Anal. Chem.*, 2003, **75**, 6544-6554.